

Shell-model description of $N \simeq Z$ $1f_{7/2}$ nuclei

F. Brandolini and C.A. Ur*

Dipartimento di Fisica dell'Università and INFN Sezione di Padova, I-35131 Padova, Italy

(Dated: October 11, 2018)

The available experimental spectroscopic data for nuclei in the middle and in the second half of the $1f_{7/2}$ shell are well reproduced by shell model calculations. For natural parity states of several odd- A nuclei a comparison of shell model calculations in the full pf configuration space with the Nilsson diagram and particle-rotor predictions shows that prolate strong coupling applies at low excitation energy, revealing multi-quasiparticle rotational bands and, in some cases, bandcrossings. Rotational alignment effects are observed only in nuclei at the beginning of the shell. Moreover, ground state bands experience a change from collective to non-collective regime, approaching the termination in the $1f_{7/2}^n$ space. Similar features are observed in the even-even $N=Z$ nuclei ^{48}Cr and ^{52}Fe and $N=Z+2$ nuclei ^{46}Ti and ^{50}Cr . In the $N=Z$ nuclei evidence of the vibrational γ -band is found. A review of non natural parity structures is furthermore presented.

PACS numbers: PACS: 21.10.-k, 21.60.Cs, 23.40.-s, 27.40.+z

I. INTRODUCTION

During the last decade an extensive theoretical work has been made to improve the quality of shell model (SM) description of the $1f_{7/2}$ nuclei, with particular care to understand the origin of their rotational collectivity [1]. The first nuclei studied in detail were ^{48}Cr [2] and ^{50}Cr [3], followed by several odd- A nuclei. One mentions in particular the mirror pair ^{49}Cr - ^{49}Mn , whose interpretation was mediated by the predictions of the particle rotor model (PRM) [4].

These theoretical advances were accompanied by a parallel experimental work at the National Laboratories of Legnaro (LNL), that exploited the advantages of the large γ -detector array GASP. The level schemes of ^{48}Cr and ^{50}Cr have been extended [5, 6] and the understanding of their collective properties was greatly increased with the help of lifetime measurements [7]. The research was thereafter extended to several nuclei in the middle of the $1f_{7/2}$, where the attention was focused on the yrast sequence of levels up to the smooth band termination in the $1f_{7/2}^n$ and $1d_{3/2}^{-1} \otimes 1f_{7/2}^{n+1}$ configuration spaces, for natural parity and unnatural parity, respectively. These structures were efficiently populated in heavy-ion induced fusion reactions. SM calculations in the full pf configuration space [1] reproduce very well the excitation energies of the observed natural parity levels and the $B(E2)$ and $B(M1)$ rates. The double shell closure at ^{56}Ni is strong enough to produce clear smooth terminations in the $1f_{7/2}$ shell, but weak enough to allow for a large mixing with the other orbitals of the pf configuration space, giving rise to collective effects which could hardly be imagined to occur in this nuclear region.

In general, low-lying levels can be classified in the framework of the prolate Nilsson diagram. The crossing of the ground state (gs) band with a sideband was

first observed in ^{50}Cr . The sideband was interpreted as a 4-qp $K^\pi=10^+$ band, originating from the simultaneous excitation of a proton from the $[321]3/2^-$ orbital to the $[312]5/2^-$ one and a neutron from the $[312]5/2^-$ orbital to the $[303]7/2^-$ one [8]. In a recent paper experimental evidence of the two 2-qp bands with $K^\pi=4^+$ for protons and $K^\pi=6^+$ for neutrons was found [9]. It was also shown that the observed mirror energy differences [10], mainly due to Coulomb energy differences (CED), are consistent with deformation alignment (strong coupling).

SM [2], cranked Hartree-Fock-Bogoliubov (CHFB) [2, 11] and cranked Nilsson-Strutinsky (CNS) [12] calculations do not confirm the origin of the backbending at $I^\pi = 12^+$ in ^{48}Cr as due to the bandcrossing inferred by projected shell model (PSM) calculations [13]. It has been rather related to the smooth termination in a $v=4$ seniority subspace [8], as suggested by the calculations of Ref. [14].

In ^{49}Cr , the backbending of the $K^\pi=5/2^-$ gs band at $19/2^-$ was similarly interpreted as a smooth termination in a $v=3$ subspace [8]. The level at 3528 keV was identified as the head of a 3-qp $K^\pi=13/2^-$ band, which is described as due to the excitation of a proton from the $[321]3/2^-$ to the $[312]5/2^-$ orbital followed by the coupling to the maximum K -value of all unpaired nucleons [15, 16]. Recently, two more members of this band were observed, as well as states belonging to the 1-qp bands based on the Nilsson orbitals $[321]1/2^-$, $[303]7/2^-$ and $[321]3/2^-$ [17]. Very interesting features were observed also for the positive parity levels. Above the 1-qp $K^\pi=3/2^+$ band built on the $[202]3/2^+$ orbital, a 3-qp $K^\pi=13/2^+$ band becomes yrast and acts to trap the decay flux towards positive parity levels of the $K^\pi=3/2^+$ band. The 3-qp band is described as due to the excitation of a proton from the $[202]3/2^+$ orbital to the empty $[312]5/2^-$ one, followed by the coupling to the maximum K of the three unpaired nucleons [15] or, in a different representation, as a $\pi d_{3/2}^{-1} \otimes ^{50}\text{Mn}(I=5, T=0)$ configuration.

In this work we shall mainly discuss natural parity

*On leave from NIPNE, Bucharest, Romania

bands in several $N \simeq Z$ odd- A and even-even nuclei pointing out further evidences of smooth terminations, multi-qp bands, bandcrossings and non-collective regime, not considered in detail in recent reviews [18, 19] and complementing the pioneering work of Ref. [4]. For this purpose the calculated static electromagnetic (em) moments provide selective probes of the underlying structure of the nucleus. It will be assumed that these observables are fully reliable, unless specifically mentioned. This is based on the good agreement achieved for level schemes and $B(E2)$ and $B(M1)$ values in most discussed nuclei and in particular in ^{49}Cr , ^{48}Cr and ^{50}Cr [7, 8, 9, 16], which are discussed here.

For reasons of clarity, the comparison will be restricted to levels up to the termination in the $1f_{7/2}^n$ configuration space even if good agreement was found also above it [19]. For the same reason odd-odd nuclei will not be discussed in spite of excellent agreement achieved [20, 21].

II. ABOUT SHELL MODEL CALCULATIONS

SM calculations will be compared with experimental level schemes taken from the last review in Nuclear Data Sheets (NDS) and most recent references.

Calculations for the natural parity levels have been made in the full pf shell using the effective interactions KB3 [1], KB3G [19] and FPD6 [22]. The KB3G interaction is just a slight modification of KB3 to better reproduce the nuclear properties approaching ^{56}Ni . Generally, their results are rather similar but in particular cases some gives better predictions. For instance, in proximity of ^{48}Cr the KB3/KB3G interaction gives excellent predictions while FPD6 is about ten percent too strong. Recently, the GXPF1 interaction has been developed for nuclei around and above ^{56}Ni [23, 24]. This interaction is rather equivalent to KB3G for the nuclei considered here but the energies are somewhat worse reproduced. This is why the KB3G interaction was adopted in our calculations. The effective interaction is made of a monopole and a multipole part. The latter one, which contains most of the structural information, is dominated by the pairing and the quadrupole terms. Calculations considering only these two multipole contributions are still made [25]. Present calculations were made assuming isospin conservation, i.e. neglecting the effect of Coulomb interaction. Bare nucleon g -factor values and effective charges (1.5 for protons and 0.5 for neutrons) were adopted. Standard PC computers with Pentium 4 CPU's and 2 GB RAM were used. The SM code ANTOINE was used, in its WEB distributed version [26, 27].

Some remarks on the consequences of configuration space truncation are worth to be mentioned here. It was observed that most of the rotational collectivity is already reproduced in a $1f_{7/2}2p_{3/2}$ subspace, where a "quasi SU(3)" scheme is valid. This means that the quadrupole deformation originates in a rather similar way

as in the SU(3) scheme in the sd shell [28]. From an empirical point of view, the main consequences of using the reduced space are that deformation is somewhat reduced and the binding energies of the lower levels are smaller so that their spacing is not fully rotational. When truncation is necessary, a limited number of nucleons s is allowed to be moved from the $1f_{7/2}2p_{3/2}$ subspace, to the $1f_{5/2}$ and $2p_{1/2}$ orbitals. Space truncation was necessary for $A \geq 42$. This truncation differs somewhat from the one commonly adopted, which counts all the particles outside the $f_{7/2}$ orbital.

III. COMPARISON OF SM AND ROTOR ESTIMATES

The SM results for em moments will be compared with the predictions of the axial rotor [29], where the configuration is described by the Nilsson diagram. The intrinsic electric quadrupole moment, Q_o , is derived from the calculated spectroscopic quadrupole moment, according to the formula:

$$Q_s = Q_o \frac{3K^2 - I(I+1)}{(I+1)(2I+3)} \quad (1)$$

The intrinsic quadrupole moment can also be derived from the $B(E2)$ values using the formula:

$$B(E2) = \frac{5}{16\pi} Q_t^2 < I_i K 20 | I_f K >^2 \quad (2)$$

where it is denoted as Q_t .

In the following we will assume $Q_t = Q_o$. Its relation with the deformation parameter β is given by the equation [30]:

$$Q_o = 1.09ZA^{2/3}\beta(1+0.36\beta) \text{ fm}^2 \quad (3)$$

For further use, we define the parameter $\beta^* = \beta(1+0.36\beta)$. The reason for this is that in literature some authors adopt the coefficient 0.16 for β inside the brackets.

Concerning the magnetic properties of odd- A nuclei, the g -factor values are expressed as:

$$g = g_R + (g_K - g_R) \frac{K^2}{I(I+1)} \quad (4)$$

and the M1 reduced probabilities are:

$$B(M1) = \frac{3}{4\pi} < I_i K 10 | I_f K >^2 (g_K - g_R)^2 K^2 \mu_N^2 \quad (5) \\ \text{(for } K \neq 1/2)$$

In the case of eq. (5) a decoupling term must be added when $K = 1/2$. These formulas have to be considered as

qualitative since, even in the extreme hypothesis of no residual interaction, K -values are mixed by the Coriolis force. This is accounted by PRM [31], but it will be shown that, generally, the mixing caused by the Coriolis force is not large in the second half of the $1f_{7/2}$ shell, so that they provide an adequate reference. It is necessary to use PRM in the first half of the shell, where the $[330]1/2^-$ Nilsson orbital is important and thus the Coriolis force gives rise to a partial Coriolis decoupling (CD).

Eq. (1) and (2) will be applied to even-even nuclei as well. The magnetic properties of the $N=Z$ nuclei ^{48}Cr and ^{52}Fe will not be considered here because they are only slightly sensitive to the nuclear structure: in self-conjugated nuclei the g -factor values approach closely the isoscalar value $\frac{g_p + g_n}{2}$, where the nucleon g -factors are the Schmidt values in the $1f_{7/2}$ shell, while $B(M1)$ values are very small. On the other hand, the magnetic properties of $N=Z+2$ nuclei have not a simple interpretation.

As previously commented, K cannot be considered a good quantum number. In fact mixings of the order of ten percent are rather often estimated, usually larger in the full pf configuration space than in the restricted $f_{7/2}p_{3/2}$ one. This makes the observation of intraband transitions difficult, because they are unfavoured by the low transition energy and it may perturb the values of em moments but, hopefully, without obscuring the basic structural effects. The mixing increases with spin due to both the decrease of the deformation and the higher level density.

The 1-qp sidebands will be not discussed in detail, since experimental data are often not precise. The Nilsson orbital assignments in the displayed level schemes are in general tentative.

A. ^{53}Fe and ^{43}Sc

For our scope, it is important to examine in detail the gs band of the nucleus ^{53}Fe , whose terminating state ($I^\pi = 19/2^-$, $E_x=3049$ keV, $\tau=3.6$ min), is dominated by a $\pi f_{7/2}^{-2}(I=6) \otimes \nu f_{7/2}^{-1}$ configuration and it is an yrast trap, as it lies four hundred keV below the yrast $15/2^-$ state. Its experimental level scheme is compared with the SM one in Fig. 1, where a $s=3$ truncation was adopted. Experimental levels were taken from NDS and a recent paper [32]. Two 1-qp sidebands are tentatively assigned. The largest contribution to the wavefunction of the yrast $1/2^-$ and $3/2^-$ levels comes from the excitation of one neutron to the $2p_{3/2}$ orbital, as expected in the case of the $[321]1/2^-$ orbital.

^{53}Fe is a very convenient testing bench to investigate how rotational collectivity builds up. In the second half of the $1f_{7/2}$ shell there is no disturbance from 2- and 4-hole configurations which are effective at the beginning of the shell [33] and moreover the $2p_{3/2}$ orbital is very active in generating deformation. ^{53}Fe is predicted to be

rather deformed in low lying states. Experimentally, this is shown by the observed fast E2 (31 Wu) transition from $5/2^-$ to $1/2^-$ which belongs to the $K=1/2$ sideband.

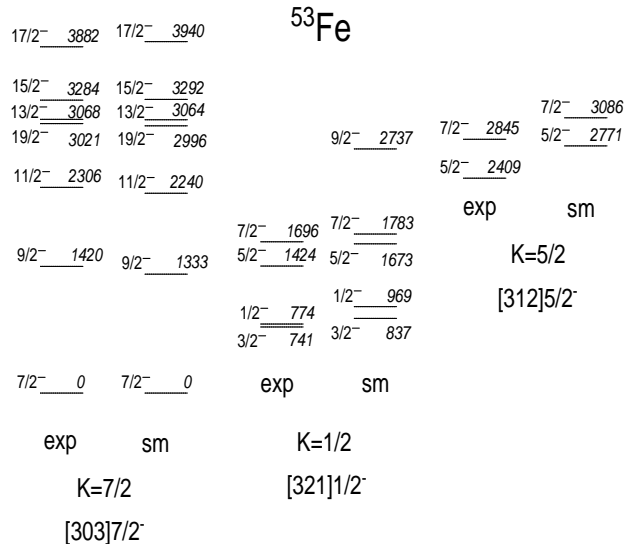


FIG. 1: Comparison of experimental negative parity levels in ^{53}Fe with SM predictions ($s=3$).

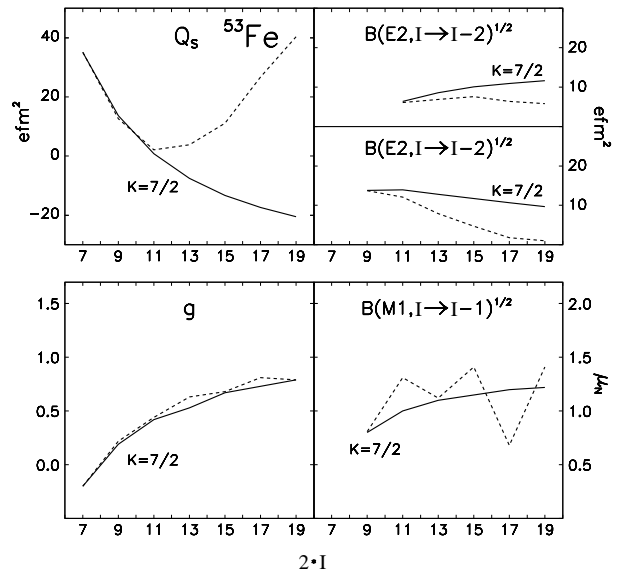


FIG. 2: Calculated em moments in the gs band of ^{53}Fe . Rotor ($\beta^*=0.19$): solid lines, SM: dashed lines.

In Fig. 2 all calculated em observables in the ^{53}Fe gs band are compared with the predictions for a prolate rotor. Differently from Ref. [4], Q_s rather than Q_o is plotted since it will be shown that eq. (1) cannot be applied in general. Furthermore, the square root of the $B(E2)$ values are reported because they are approximately proportional to the deformation as the Q_s values do. The Q_s value of the gs state is predicted to be large and positive, as expected for a prolate $K=7/2$ band with $\beta^* \simeq$

TABLE I: ^{43}Sc .

I	E_x keV	E_{sm} keV	Q_s efm ²	$B(E2, \Delta I=1)$ e ² fm ⁴	$B(E2, \Delta I=2)$ e ² fm ⁴	E_{prm} keV	Q_s efm ²	$B(E2, \Delta I=1)$ e ² fm ⁴	$B(E2, \Delta I=2)$ e ² fm ⁴
7/2 ⁻	0	0	-18	-	-	0	-8	-	-
9/2 ⁻	1883	1999	-11	14	-	1905	-27	14	-
11/2 ⁻	1830	1816	-17	16	26	1570	-13	8	27
13/2 ⁻	3958 ^a	3445	-10	5	13	5364	-9	8	32

^aRef. [34]

0.19. Calculated Q_s and $B(E2)$ values agree with rotor predictions only at low spins up to 11/2, while the typical $I(I+1)$ spectrum has not room to get evident. What occurs above 11/2 will be discussed later. In the $1f_{7/2}^n$ space cross-conjugate nuclei should have identical level scheme, while, experimentally, large difference are observed, pointing to different configuration mixing and collective properties. The predicted level scheme for the $\pi^{-2}\nu^{-1}$ ^{53}Fe is in fact substantially different from that of its cross-conjugate $\pi^1\nu^2$ ^{43}Sc . In both cases the gs level is 7/2⁻, but in ^{43}Sc a large signature splitting (SS) is observed. Another striking difference is that the $B(E2)$ values of the transition from the yrast level 9/2⁻ to the 7/2⁻ in ^{43}Sc and ^{53}Fe are 13.6 and 217.2 efm², respectively. The latter is a fingerprint of the prolate collectivity in ^{53}Fe , since in a $1f_{7/2}^3$ space only one third of this value is predicted. The properties of ^{43}Sc , on the other side, can be roughly described by PRM predictions, assuming a slightly prolate shape with $\beta^*=0.10$, which predict rotational alignment in the gs band built on the [330]1/2⁻ Nilsson orbital. SM predictions are compared with PRM predictions in Table I. There is some correspondence, in spite of the naive description. It has to be remarked, however that SM calculations are not good in ^{43}Sc , because 2h- and 4h-configurations strongly mix at low spin in nuclei close to ^{40}Ca [33]. This does not occur in the isotope ^{47}Sc with $\pi^1\nu^{-2}$, where good agreement is achieved by SM [4]. Both ^{43}Sc and ^{53}Fe , as in general $1f_{7/2}$ nuclei, are described with a prolate shape.

The different structure of the cross-conjugate nuclei is confirmed by the contribution of the $1f_{7/2}^n$ configuration (expressed in percentage) to the states along the gs band. For the levels with spin 7/2, 9/2, 11/2, 13/2, 15/2, 17/2 and 19/2 the contributions are 79, 96, 72, 95, 78, 88 and 96 in ^{43}Sc and 56, 54, 58, 60, 63, 60 and 64 in ^{53}Fe . The staggering of the values in ^{43}Sc is related to the observed SS, where the 7/2⁻ ground state has the favoured signature. These numbers provide, moreover, a qualitative explanation for the inversion between the 15/2⁻ and 19/2⁻ observed in ^{53}Fe . The level scheme calculated in the $1f_{7/2}^{\pm 3}$ space predicts the inversion, as a consequence of the very attractive $V_{pn}(I=7, T=0)$ term. The inversion is preserved in ^{53}Fe because the contribution of $1f_{7/2}^{-3}$ is similar in the two states, while in ^{43}Sc the $1f_{7/2}^3$ contribution is about 20 % larger for the 19/2⁻, so that the 15/2⁻ has an additional binding energy, that lowers

it below the 19/2⁻ level. More than one third of the upper orbital occupation refers to the $2p_{3/2}$ one, which give rise to large quadrupole terms.

CD is expected to be large at low spin if the gs band is based on the [330]1/2 orbital as in ^{43}Sc , it is noticeable for the [321]3/2⁻ orbital, giving rise to partial rotational alignment (RAL), and nearly negligible for the orbitals [312]5/2⁻ and [303]7/2⁻. It becomes important in the case of the intruder orbital [440]1/2⁺, originating from the spherical $1g_{9/2}$ orbital.

As shown in Fig. 2, the Q_s values of the ^{53}Fe gs band start to increase above $I^\pi = 11/2^-$, reaching at the terminating spin 19/2⁻ a maximum of 42.9 efm², calculated with $s=4$. This value may be somewhat larger in full pf calculations. This is consistent with its hole-like nature, to which a prolate non-collective shape pertains, being made of three valence nucleon-hole. In a semiclassical description $Q_s = Q_o$ and thus $\beta^* \simeq 0.11$ is derived from eq. (3). Since $Q_s = 25$ efm² is predicted in the $1f_{7/2}^n$ space, one infers that the terminating state is strongly polarised by the upper orbitals, getting a strong enhancement of the non-collective prolateness. Its terminating nature is confirmed by the fact that yrast 21/2⁻ and 23/2⁻ levels are predicted more than 4 MeV above it. The Q_s value is stable upon large variations of the binding energies of the upper orbitals. It would be of great interest to measure the Q_s value of the 19/2⁻ terminating state.

In a $\beta - \gamma$ plane the shape changes from $\gamma \simeq 0$ at the bottom of the gs band to $\gamma \simeq -120$ at its termination (Lund convention). While it is commonly accepted that the terminating states are non-rotational, it is not trivial to explain how the nuclear shape evolves along the gs band. This problem has been commonly addressed with the configuration dependent CNS approach [35], as recently made for ^{50}Mn , where the low-lying bands terminate as prolate non-collective [36]. One may question whether a meanfield description as that of CNS can describe accurately a system with few valence particles or holes. One should find that in few steps the nucleus changes in sequence to triaxial collective, oblate collective and finally prolate non-collective shapes. It seems more realistic to imagine a rapid change from prolate collective to prolate non-collective, because an oblate collective shape is likely inhibited by the simple shell model structure. On the other hand, it is known since a long time that the single particle structure of a prolate nucleus

may favour a prolate non-collective shape [37]. More arguments for a sudden shape change will be presented in the discussion of other nuclei.

The evolution of Q_s values approaching the terminating spin $19/2^-$ is certainly incompatible with rotational alignment, elsewhere proposed [38], because a negative value of Q_s would be expected in that case, as one has to put a large value of I and a small one for K in eq. (1).

In the past, the non-collective prolate shape at the band termination was alternatively interpreted as a high- K collective prolate shape [39]. This misunderstanding originates from the large overlap of the two wave functions: in fact a $I=K=19/2$ state is oriented spacially almost in the same manner, where $Q_s=0.74Q_o$, according to eq. (1). The substantial physical difference is that the non-rotational state is a terminating one, while the hypothetical $K=19/2$ state would be a bandhead. The latter description is clearly excluded by the observation that Q_s increases gradually with the level spin so that also previous levels should have a dominant high- K character, which is unrealistic.

In Table II the predictions of Q_s values for several terminating states in $N \simeq Z$ nuclei are compared with $f_{7/2}^n$ predictions. Calculations were made in the full pf configuration space, except for $52 \leq A \leq 54$ and $A=55$ where $s=4$ and $s=3$ truncations were assumed, respectively. Obviously, in the Table a 4-hole configuration coincides with a 4-particle one. These states are generally supposed to have nearly pure $f_{7/2}^n$ configuration, but this turns out to be not true approaching the end of

the shell, where configuration mixing becomes important. One observes that a negative value of Q_s is calculated for ^{48}Cr , where 0 is expected in the $1f_{7/2}$ space. Similarly, a negative offset applies to neighbouring nuclei. The scale factor of Q_s for the single proton-hole nucleus ^{55}Co in the $f_{7/2}^n$ is $(2j-1)/(2j+1) < r^2 >$ [29]. It is peculiar that $\nu^{-2}\pi^{-1}$ and $\nu^{-1}\pi^{-2}$ configurations have a similar Q_s value.

The experimental g -factor value of the $19/2^-$ level in ^{43}Sc is known to be 0.329(1), that of the 6^+ level in ^{54}Fe is 1.37(3) and finally the g -factor of the single hole $7/2^-$ level in ^{55}Co is 1.378(1). Thus, all experimental values known with high precision agree with the SM predictions of Table II.

As previously stated, the interaction KB3G has been adopted in Table II. Calculations made with the GXPF1 one are nearly equivalent, while the FPD6 interaction would predict a mixing about 30% higher for the terminating states approaching shell closure, accompanied by up to 20 % larger $B(E2)$ rates. It is a critical point the capability of the effective interaction to get good results in proximity of the shell closure. The experimental value $B(E2, 6^+ \rightarrow 4^+) = 39.7(5) \text{ efm}^2$ in ^{54}Fe provides a test for the effective interactions. The interactions KB3G, GXPF1 and FPD6 gives $B(E2, 6^+ \rightarrow 4^+)$ values 40.3, 40.7 and 46.7 efm^2 , using a $s=4$ truncation. The $1f_{7/2}^n$ prediction is 23.1 efm^2 , independently from the adopted interaction. It turns out that the FPD6 interaction overestimates the $B(E2)$ value by about 20 %.

The internal consistence of SM predictions is confirmed by the g -factor predictions for the terminating $19/2^-$ level. It can be estimated with the additivity rule:

TABLE II: Q_s and g -factor values of terminating states.

Nuclide	config.	I^π	$P(f_{7/2})$ %	Q_s efm ²	$Q_s(f_{7/2})$ efm ²	g_{sm}	g_{emp}
^{55}Co	π^{-1}	$7/2^-$	62.6	24.1	17.5	1.350	1.38
^{55}Ni	ν^{-1}	$7/2^-$	"	14.8	5.8	-0.271	-0.30
^{54}Fe	π^{-2}	6^+	61.1	27.2	19.8	1.337	1.38
^{54}Ni	ν^{-2}	6^+	"	18.9	6.6	-0.256	-0.30
^{53}Fe	$\pi^{-2}\nu^{-1}$	$19/2^-$	60.7	42.9	25.5	0.770	0.80
^{53}Co	$\pi^{-1}\nu^{-2}$	$19/2^-$	"	43.1	23.8	0.318	0.28
^{52}Fe	$\pi^{-2}\nu^{-2}$	12^+	60.9	47.1	26.1	0.547	0.54
^{51}Mn	$\pi^{-3}\nu^{-2}$	$27/2^-$	68.4	32.7	18.6	0.646	0.65
^{51}Fe	$\pi^{-2}\nu^{-3}$	$27/2^-$	"	39.4	23.5	0.446	0.43
^{50}Cr	$\pi^{-4}\nu^{-2}$	14^+	75.3	7.1	6.4	0.668	0.68
^{50}Fe	$\pi^{-2}\nu^{-4}$	14^+	"	22.3	19.3	0.421	0.40
^{49}Cr	$\pi^{-4}\nu^{-3}$	$31/2^-$	88.9	1.6	4.0	0.586	0.57
^{49}Mn	$\pi^{-3}\nu^{-4}$	$31/2^-$	"	9.8	12.0	0.503	0.51
^{48}Cr	$\pi^4\nu^4$	16^+	89.4	-6.7	0	0.553	0.54
^{47}V	$\pi^3\nu^4$	$31/2^-$	87.5	-19.2	-12.0	0.534	0.51
^{47}Cr	$\pi^4\nu^3$	$31/2^-$	"	-14.4	-4.0	0.549	0.57
^{46}Ti	$\pi^2\nu^4$	14^+	86.7	-24.2	-19.3	0.449	0.40
^{46}Cr	$\pi^4\nu^2$	14^+	"	-18.8	-6.4	0.638	0.68
^{45}Ti	$\pi^2\nu^3$	$27/2^-$	90.0	-26.8	-23.5	0.471	0.43
^{45}V	$\pi^3\nu^2$	$27/2^-$	"	-25.8	-18.6	0.616	0.65
^{44}Ti	$\pi^2\nu^2$	12^+	94.3	-27.7	-26.1	0.545	0.54
^{43}Sc	$\pi^1\nu^2$	$19/2^-$	96.1	-23.1	-23.8	0.330	0.28
^{43}Ti	$\pi^2\nu^1$	$19/2^-$	"	-26.3	-25.5	0.765	0.80

$$g = \frac{g_p + g_n}{2} + \frac{g_p - g_n}{2} \frac{I_p(I_p + 1) - I_n(I_n + 1)}{I(I + 1)} \quad (6)$$

for a pure $\pi f_{7/2}^{-2}(I = 6) \otimes \nu f_{7/2}^{-1}$ configuration. If one assumes $g_n = -0.30$ and $g_p = 1.38$ in the $1f_{7/2}$ orbitals, instead of the Schmidt values of -0.547 and 1.655 , respectively, one gets the mean reproduction of SM values of Table II. These effective values, which roughly account for configuration mixing, will be adopted in semiclassical considerations. In the case of the mirror nucleus ^{53}Co , the isovector part, i.e. the second addendum in eq. (6), changes sign. Looking to Table II we see that the SM isoscalar part agrees with the empirical value of 0.54, calculated as the average of the values for a mirror pair.

The slope of the g values at low spin follows rather closely a rotor behaviour, where the asymptotic value at high spins is not the usual $g_R \simeq 0.5$, assumed for a similar and large number of neutrons and protons, but the curve is adjusted to $g=0.77$ at $I = 19/2$, according to eq.(6), because only two proton-holes and one neutron-hole are active. The slope of $B(M1)$ is also consistent with a rotor behaviour, apart from a staggering approaching termination, which is characteristic of a $1f_{7/2}^{-3}$ description.

In summary, ^{53}Fe can be considered a paradigm of the

fragility of the collective rotation in $1f_{7/2}$ nuclei and of the intrinsic change of regime along the gs band.

Also ^{43}Sc is understood in proximity of the termination. There the configurations become particle-like, so that a non-collective oblate configuration is expected, to which also a negative Q_s value pertains. It must be stressed, therefore, that an ambiguity arises for nuclei at the beginning of the shell, since a negative Q_s value is predicted for them both before and after the phase transition.

B. ^{49}Cr

The next nucleus to be examined is the $N=Z+1$ ^{49}Cr , which has been studied in detail in Refs. [15, 16, 17]. A partial level scheme of ^{49}Cr is shown in Fig. 3, up to the termination at $31/2^-$. Only the lower members of the 1-qp sidebands are reported and, approaching the termination, only states with prevailing $1f_{7/2}$ configuration. Few levels were added with respect to Refs. [15, 16], which were observed in a recent experimental work [17], where also a detailed comparison with PRM was made. Calculated levels are also organised in bands.

SM calculations are able to reproduce well the observed levels. The gs band is described at low spins as a $K^\pi=5/2^-$ band based on the $\nu[312]5/2^-$ Nilsson orbital [4, 16]. The 1-qp sidebands with $K=1/2$, $7/2$ and $3/2$ are described with Nilsson orbitals $[321]1/2^-$, $[303]7/2^-$ and $[321]3/2^-$, respectively. Only the first two are reported in Fig. 3. A 3-qp band with $K^\pi=13/2^-$ is also observed, which is predicted by breaking a $[321]3/2$ proton pair, lifting one of them into the $[312]5/2^-$ and coupling the three unpaired particles to the maximum K value.

The measured lifetimes lead to an initial β^* value of 0.28 for the gs band, which was adopted in Fig. 4 where the em properties are plotted and compared with the rotational model. The Q_s value of the $K^\pi=13/2^-$ bandhead is 51.2 efm^2 , which corresponds to $\beta^*=0.24$. The smaller deformation is reasonable owing to the high spin, which reduces the number of possible interacting nucleons in the $2p_{3/2}$ orbital and thus the collectivity. Moreover some mixing is also present.

In the same figures also a 5-qp band with $K^\pi=23/2^-$ is reported which is obtained by breaking also a $[321]3/2$ neutron pair and lifting one of them to the $[303]7/2^-$ orbital. It is merely incipient since it terminates at the common termination $31/2^-$ ($Q_s = 1.6 \text{ efm}^2$). The calculated Q_s moment of the $K^\pi=23/2^-$ bandhead is 38.8 efm^2 , corresponding to a $\beta^*=0.16$ value. The yrare $25/2^-$ state is mixed so that it decays to the yrast $23/2^-$ state with a fast M1.

The magnetic moment of the $I^\pi=K^\pi=13/2^-$ state is given semiclassically by the sum of the longitudinal component along the total spin. In the $1f_{7/2}^n$ space, taking $\cos\theta = K/j$ one gets $g = \mu/I \simeq 2/13[1.38 \cdot (3/2 + 5/2) - 0.3(5/2)]$, so that the g -factor of the $13/2^-$ level

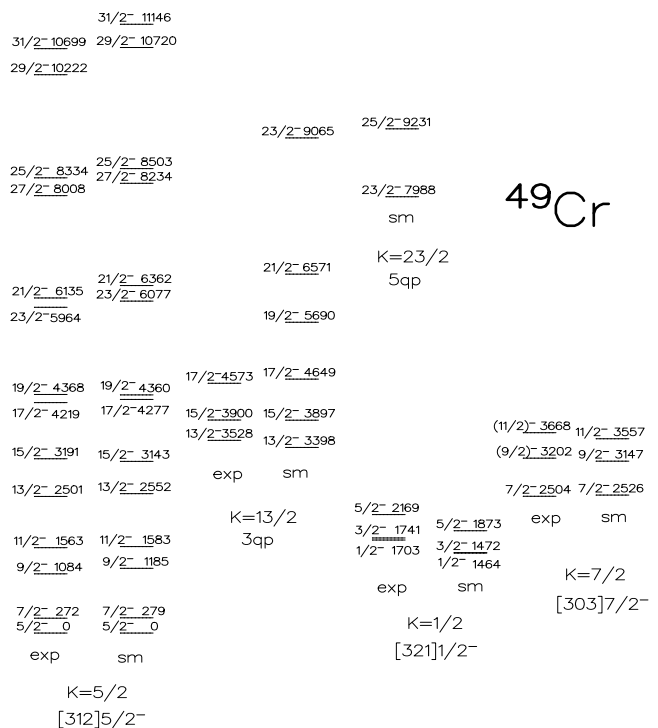


FIG. 3: Comparison of experimental negative parity levels in ^{49}Cr with SM predictions.

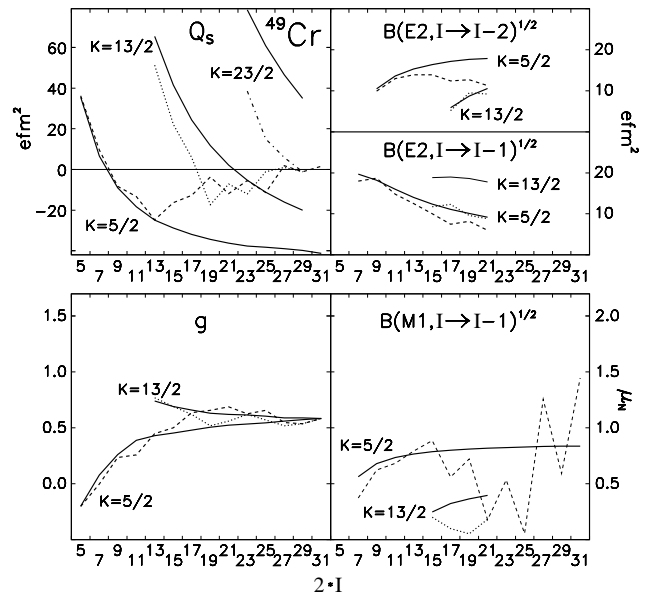


FIG. 4: Calculated em moments in ^{49}Cr . Rotor ($\beta^*=0.28$): solid line. SM: dashed ($K=5/2$) and dotted ($K=13/2$) lines.

is $g=0.74$, in agreement with the SM value of 0.77. The curves of g and $B(M1)$ adopt such empirical values. It has to be noted that in Fig. 3 some SS is observed at low spin, whose size is not reproduced by PRM and CSM [40].

Above the backbending at $19/2^-$ the SS of the gs band

becomes so large that the ordering of spin values is inverted. This indicates a sudden change of regime, which cannot be associated to a bandcrossing, neither experimentally, nor theoretically [15].

The low spin part of Fig. 4 is reproduced without triaxiality. From the Q_s values it results that the collective rotation of the ^{49}Cr gs band starts to be severely damaged above $I^\pi = 13/2^-$. In fact, at low spin they follow the rotor predictions getting rapidly negative, according to eq. (1), but they start to increase around $13/2^-$, approaching zero at $I^\pi = 19/2^-$, presumably due to the influence of the $v=3$ termination.

This interpretation is confirmed by the g -factor curve, adjusted at $I=31/2$ to the empirical value 0.57, obtained from the additivity rule (the SM value is 0.59). The SM g -factor ranges around 0.65 at spin $19/2^-$, which is larger than the rotor value of 0.53, while it is at the halfway to the value of 0.79 for the termination of $v=3$ states.

A similar effect occurs apparently in $1g_{9/2}^n$ nuclei too. The gs band of ^{93}Pd , with a configuration $\pi^{-4}\nu^{-3}$, has a backbending at the $25/2^+$ [41], which can be interpreted as a termination in a $v=3$ subspace. Its gs band appears to be little collective, indicating that approaching the $N=Z=50$ shell closure the polarising action of the $2d_{5/2}$ orbital on the $1g_{9/2}$ one is less effective than that of the $2p_{3/2}$ orbital on the $1f_{7/2}$ one, because of the larger energy gap between the orbitals.

It appears rather questionable to speak of rotational bands above $I \simeq 15/2$ since the bands start to be strongly mixed and single particle features get evident. In fact, the staggering of $B(M1)$ values approaching band termination is a $1f_{7/2}^n$ phenomenon [42], which cannot be reproduced by a deformed meanfield model.

C. ^{51}Mn

Experimental levels, $B(E2)$ and $B(M1)$ values of the $N=Z+1$ nucleus ^{51}Mn have been recently found to agree with the SM calculations [19]. The gs band is interpreted with the same Nilsson configuration $[312]5/2^-$ as ^{49}Cr , while the termination now occurs at $27/2^-$. The experimental level scheme of ^{51}Mn shown in Fig. 5 includes data from NDS and the very recent Ref. [43]. The $K^\pi=5/2^-$ gs band resembles that of ^{49}Cr , apart from a larger SS, up to the backbending at $17/2^-$, pointing to a similar deformation. Calculated em observables are plotted in Fig. 6. The larger SS is correlated with the staggering of $B(M1)$ and g -factor values. CD could produce staggering only at rather high spin, while the observed one starts early. In CSM such early staggering is considered an indication of triaxiality, associated with a $\gamma < 0$. The larger SS in ^{51}Mn with respect to ^{49}Cr can be interpreted as a sign of substantial triaxiality.

Staggering was observed also in the CED values [44, 45], which thus may be related with triaxiality. In spite of that the axial rotor formulas with $\beta^* = 0.27$ reproduce qualitatively the SM values for Q_s and $B(E2)$ at low

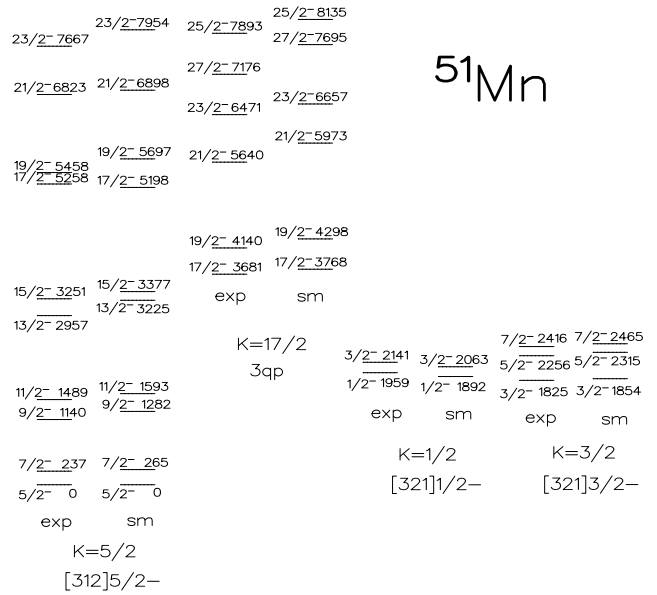


FIG. 5: Comparison of experimental negative parity levels in ^{51}Mn with SM predictions.

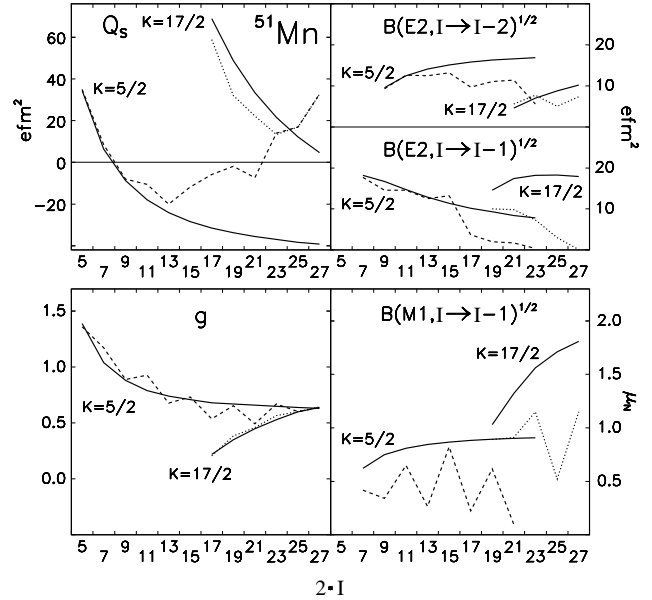


FIG. 6: Calculated em moments in ^{51}Mn . Rotor ($\beta^*=0.26$): solid lines, SM: dashed ($K=5/2$) and dotted ($K=17/2$) lines.

spins. It has to be noted that above $15/2^-$ the $B(E2)$ values for $\Delta I = 1$ transitions become very small. The calculated gs g -factor is 1.359 in agreement with the experimental 1.427 and not far from the effective value for a $1f_{7/2}$ proton.

The 3-qp band is produced by breaking a $[312]5/2^-$ neutron pair, lifting one of them into the $[303]7/2^-$ and coupling the three unpaired particles to the maximum K value. The interpretation of the yrast $17/2^-$ level as a $K^\pi=17/2^-$ bandhead was already proposed [9, 46] to explain the observed anomaly of CED val-

ues starting at $I=17/2$. It is confirmed by the predicted large Q_s value of 56.3 efm^2 , which corresponds to $\beta^* = 0.22$, according to eq. (1). This estimate may be lowered by some configuration mixing. Moreover, the low SM value of its g -factor (0.206) is related to the fact that now the 3-qp state is formed by one $K=5/2$ proton and two neutrons with $K=5/2$ and $7/2$, respectively. Semiclassically, as previously made in ^{49}Cr , $g = \mu/I \simeq 2/17[1.38 \cdot 5/2 - 0.30(3/2 + 5/2)]$, resulting in a g -factor of 0.26 for the $17/2^-$ level.

The calculated yrast level $19/2^-$ is assigned to the $K=17/2$ band in virtue of its em properties. The $B(E2)$ value of the transition to yrast $17/2^-$ level is large, as expected for an intraband transition, while the one to the yrast $15/2^-$ is small. Its g -factor is 0.39, much smaller than the rotor value of 0.60, obtained adjusting the rotor curve to the empirical value of 0.63 at $27/2^-$ (the SM value is 0.64).

The yrare $17/2^-$ level belongs to the gs band since its E2 decay to the yrast $13/2^-$ is favoured. The yrare $19/2^-$ state was not observed. It is predicted to have $g=0.67$, higher than the rotor value of 0.58 and at the halfway to the $\nu=3$ value of 0.79. Its Q_s value is slightly positive.

The gs band level spacing and Q_s values change rapidly above the $13/2^-$ level, pointing to a change of regime as in ^{49}Cr , but, while in the case of ^{51}Mn the SS decreases in ^{49}Cr it increases. The reason of the different behaviour is not understood. The change of regime is signalled also by the sudden change of Q_s and $B(E2, I \rightarrow I-1)$ values above $17/2^-$.

The positive value of Q_s at the terminating level $27/2^-$ (32.7 efm^2) is due to the non-collective prolate shape of the $\pi^{-3}\nu^{-2}$ configuration. The corresponding β^* is 0.09. The two bands with $K=5/2$ and $17/2$ loose collectivity with increasing spin and the Q_s value becomes for both positive.

As for ^{53}Fe , the observed positive Q_s value at $23/2^-$ and above, it is incompatible with rotational alignment, since the Q_s value would be expected to be negative in that case.

Yrast high- K bands of natural parity can occur only in the second half of the $1f_{7/2}$ shell because one needs to deal with high- K Nilsson orbital. In fact, the reason why the $K^\pi=17/2^-$ crosses the gs band, while the $K^\pi=13/2^-$ band in ^{49}Cr does not, is that their excitation energy is similar, but the spin values are higher in the former case.

Applying the Nilsson diagram to look for a possible 5-qp band as in ^{49}Cr , one gets $K^\pi=27/2^-$, but $I^\pi = 27/2^-$ is the terminating state, so that a 5-qp band does not exist in ^{51}Mn .

D. ^{51}Cr

The $N=Z+3$ nucleus ^{51}Cr has been recently discussed [19], but the bandcrossing of the gs band was not recognised. The gs band is based in this case on the Nilsson orbital $\nu[303]7/2^-$. The experimental levels, taken from

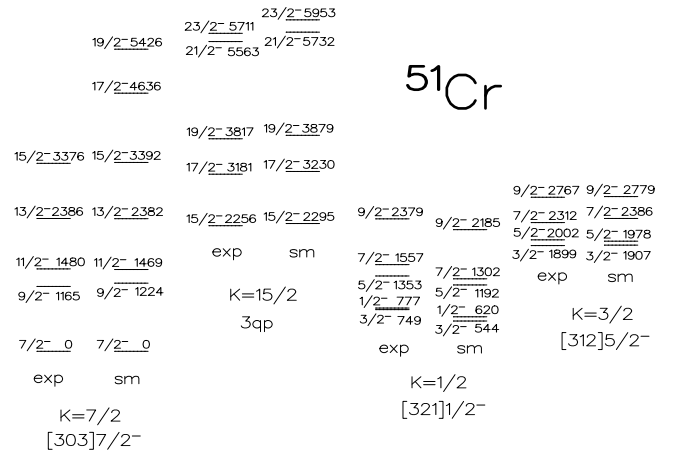


FIG. 7: Comparison of experimental negative parity levels in ^{51}Cr with SM predictions ($s=3$).

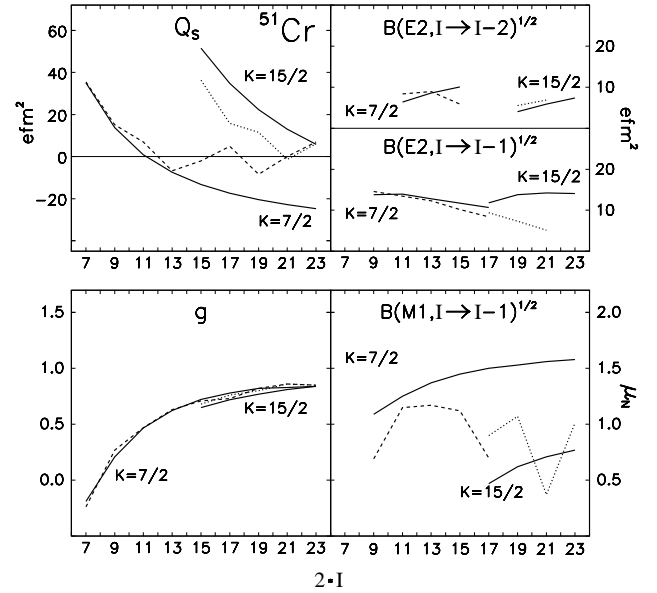


FIG. 8: Calculated em moments in ^{51}Cr . Rotor ($\beta^*=0.21$): solid lines, SM: dashed ($K=5/2$) and dotted ($K=17/2$) lines.

NDS, are displayed in Fig. 7 where they are compared with SM calculations up to the termination at $23/2^-$ ($Q_s=6.9 \text{ efm}^2$). Since its configuration is $\pi^{-4}\nu^{-1}$, the positive value is due to the neutron hole configuration, which is larger than that of the ν^{-3} configuration in ^{49}Cr . The calculated levels reported here were obtained with a $s=3$ truncation. Calculations were made also in full pf configuration space, but a worse average agreement by about $\simeq 50 \text{ keV}$ was obtained, possibly pointing to a somewhat too large contribution of the $1f_{5/2}$ orbital. Relevant SS occurs at the yrast $9/2^-$ level, but it decreases above, in contrast with ^{49}Cr . The deformation parameter at low spins is $\beta^*=0.21$, much smaller than in ^{48}Cr .

The yrast $15/2^-$ level is interpreted as the head of the 3-qp band obtained by lifting one proton from the

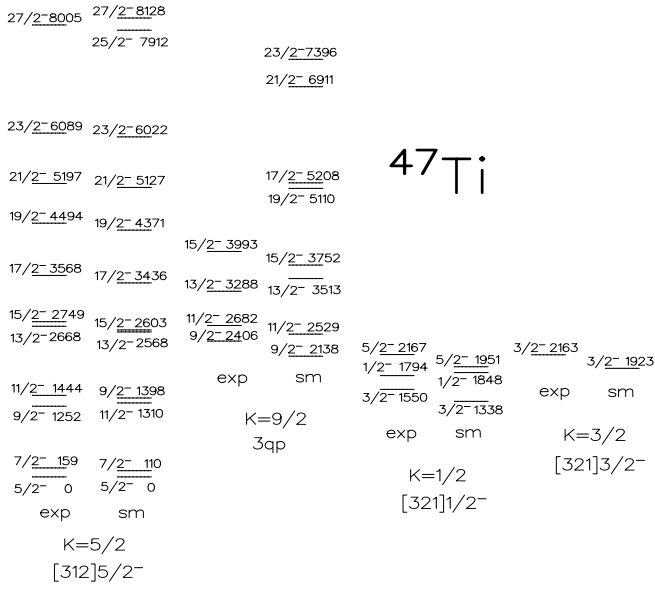


FIG. 9: Comparison of experimental negative parity levels in ^{47}Ti with SM predictions.

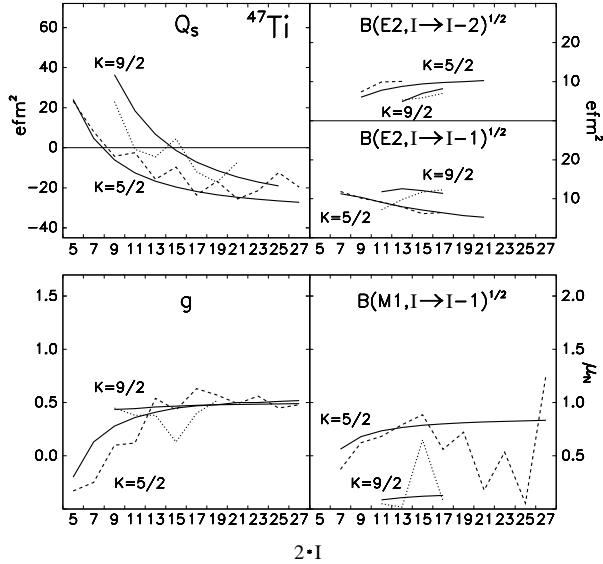


FIG. 10: Calculated em moments in ^{47}Ti . Rotor ($\beta^*=0.22$): solid lines, SM: dashed ($K=5/2$) and dotted ($K=17/2$) lines.

$[321]3/2^-$ orbital to the $[312]5/2^-$ one and coupling the three unpaired nucleons to the maximum value of K . The empirical g -factor is $g = \mu/I \simeq 2/15[1.38(3/2 + 5/2) - 0.30 \cdot 7/2] = 0.60$, while the SM value is 0.69.

The em observables are plotted in Fig. 8 and they resemble qualitatively the ones of ^{49}Cr .

The g -factor values of both bands converge at $I=23/2$ to the empirical value 0.87 (the SM value is 0.85). The agreement of SM values with rotor prediction is remarkable.

E. ^{47}Ti

In the $N=Z+3$ nucleus ^{47}Ti the gs band is based on the $\nu[312]5/2^-$ orbital as in ^{49}Cr and shows relevant SS as in ^{51}Mn . Levels were taken from NDS. As shown in Fig. 9 no bandcrossing occurs along the gs band, since the $K=9/2$ 3-qp band, resulting from the lifting of one proton from the $[321]1/2^-$ orbital to the $[312]3/2^-$ one, is largely non yrast. The semiclassical g -factor of the sideband head is $g = \mu/I \simeq 2/9[1.38(1/2 + 3/2) - 0.30 \cdot 5/2] = 0.45$ while the SM value is 0.44. The terminating Q_s value is -19.6 efm^2 , showing that the shape associated to the π^2 configurations largely prevails on that of the ν^{-3} one. This occurs also in a restricted $f_{7/2}^n$ space. The empirical g -factor value at termination is 0.45, in agreement with the SM value 0.48.

^{47}Ti has been discussed in detail in Ref. [4] as a distinct case of incipient rotational collectivity, since the Q_s values follow the expectation for a rotating prolate nucleus nearly up to the termination at $I=27/2$, but this is illusory since approaching termination, the negative value of Q_s is associated to an oblate non-collective shape and not to a prolate collective one. The values of Q_s displayed in Fig. 10 do not reveal the change of regime, which is, however, signalled by the sudden decrease of SS above $15/2^-$, as in ^{51}Mn and ^{51}Cr . The nucleus is not much deformed, so that configurations are quite mixed. The particularly large perturbation of the sideband at $15/2^-$ can be interpreted as due to the mixing with a 3- ν configuration. In this case a $K=15/2^-$ band results from the parallel coupling of neutron orbitals $[321]3/2^-$, $[312]5/2^-$ and $[303]7/2^-$. This produces both the positive value of Q_s and the small value of g . Similarly, the inversion of sideband levels $19/2^-$ and $17/2^-$ may be caused by the interaction with a $19/2^-$ 5-qp band, which is obtained by further breaking a neutron pair. The SS at low spins presents a problem since PRM and CSM with $\gamma \leq 0$ cannot explain its entire size. This may point to some limits of the meanfield approximation.

F. ^{47}V and ^{49}V

Large SS at low spin is observed in the odd V isotopes ^{45}V , ^{47}V and ^{49}V . Their level schemes are basically similar at low excitation energies, as they are all based on the $[312]3/2^-$ Nilsson orbital, giving rise to a $K^\pi=3/2^-$ band. The three isotopes are characterized by having very close yrast $3/2^-$, $5/2^-$ and $7/2^-$ levels, even if the ordering changes. This can be explained by a sensible RAL, induced by the mixing with the orbital $[330]1/2^-$ caused by pairing, which is reasonably well reproduced by PRM calculations. Termination occurs at $27/2^-$ in ^{45}V and ^{49}V , while at $31/2^-$ in ^{47}V . The 3-qp band is expected to have $K=7/2^-$, $11/2^-$ and $15/2^-$ in ^{45}V , ^{47}V and ^{49}V , respectively.

The level scheme of the $N=Z+1$ nucleus ^{47}V is shown in Fig. 11. The gs band has been discussed in Ref. [16],

version. According to Ref. [4] the g -factor values around $19/2^-$ reflect a $v=3$ termination but, contrarily to ^{49}Cr , the change of regime seems to interfere with the effects of $v=3$ termination in such a way that the backbending at $I=19/2$ is not observed. In this nucleus it is particularly difficult to assign side levels to 1-qp bands, since there is no regularity. The $K=1/2$ band is denoted by $[330]1/2^-$. The experimental $5/2$ level at 2176 does not have a calculated counterpart.

Fig. 13 shows that the level scheme of the $N=Z+3$ nucleus ^{49}V is well predicted by SM calculations and it presents analogies with that of ^{47}V . At the termination the Q_s value is -8.5 efm^2 , showing that the proton hole shape prevails. It has the largest SS among the three isotopes and its gs band is expected to be crossed by a $K^\pi=15/2^-$ 3-qp band, which is observed experimentally. Its bandhead is the yrare $15/2^-$ with $Q_s = 33.0 \text{ efm}^2$, while the member with $I=17/2$ is yrast. The larger SS is probably related with triaxiality, reflecting a high configuration mixing among Nilsson configurations. For this reason a limited number of levels is reported in Fig. 14. For sidebands only theoretical predictions are displayed in this case. The g -factor of the $K=15/2$ band head is predicted to be $g = \mu/I \simeq 2/15[1.38 \cdot 3/2 - 0.30(5/2 + 7/2)] = 0.04$, which greatly differs from the SM value of 0.34, indicating mixing effects, which apparently also lower its Q_s value in Fig. 14.

The empirical g -factor value at the termination is 0.63, in agreement with the the SM value 0.66.

The level schemes of ^{45}V and of its mirror ^{45}Ti are identical, apart for Coulomb effects. Their level schemes are somewhat perturbed at low spin by intruder $2h^-$ and $4h^-$ configurations. They will not be further discussed here because their level schemes are not sufficiently well known to bring relevant new information.

G. ^{48}Cr

In the last ten years ^{48}Cr has been addressed by several theoretical studies as its understanding is considered to be of strategic importance. An updated experimental level scheme is reported in Fig. 7. Yrast levels were taken from Ref. [7], while yrare levels essentially from a recent work [47], where spin-parity assignments were not precisely determined. It is assumed that all experimental sidelevels in Fig. 15 have positive parity, on the basis of the following argument: in ^{48}Cr a negative parity band with $K^\pi=4^-$, whose band head is at 3532 keV, was determined in Ref. [7], where it was described as the coupling of the $[202]3/2^+$ orbital with the $[312]5/2^-$ one. This band was well reproduced by SM calculations, which predict at an energy more than one MeV higher the $K^\pi=1^-$ band originating from the antiparallel coupling. The reliability of these predictions is stressed by the fact that the lowest terms of both bands were observed and correctly reproduced in ^{50}Cr [46].

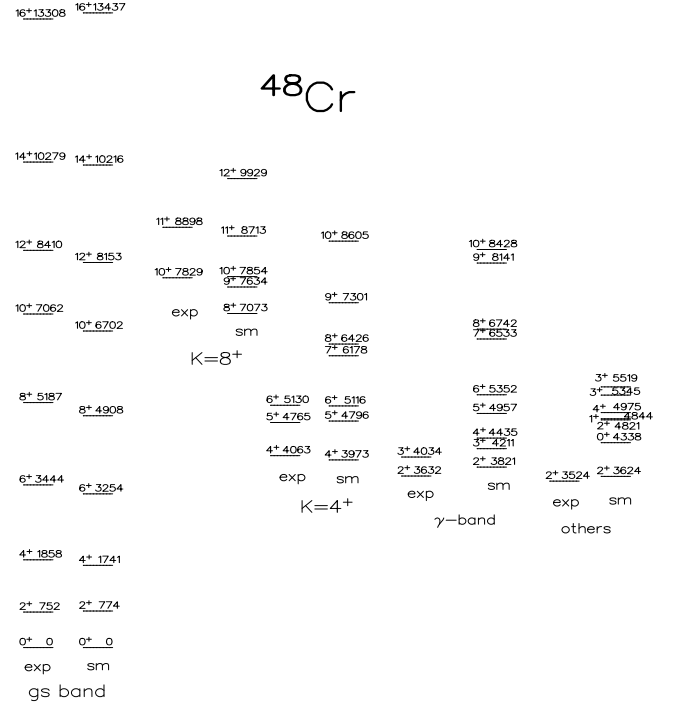


FIG. 15: Comparison of experimental positive parity levels in ^{48}Cr with SM predictions.

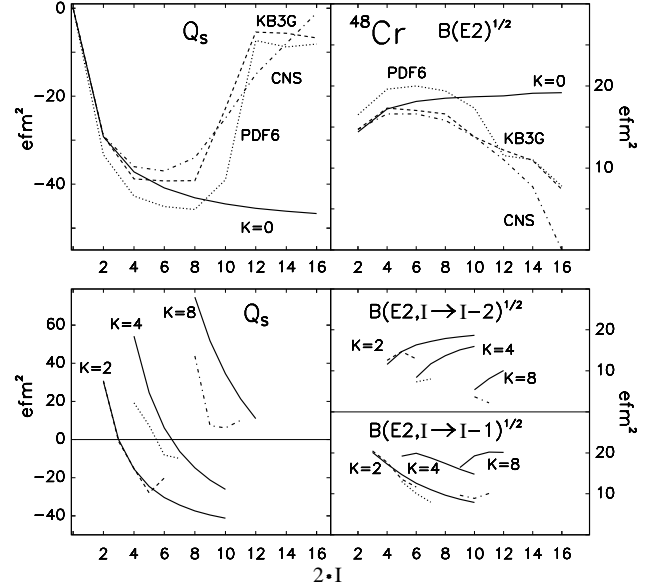


FIG. 16: Upper panels) Comparison of rotor ($\beta^*=0.31$) estimates with some SM predictions for the gs band in ^{48}Cr . Lower panels) Calculated em moments in ^{48}Cr . Rotor: solid lines, SM: dashed ($K=2$), dotted ($K=4$) and dot-dashed ($K=8$) lines.

The observed lowest sidelevels [47] are tentatively assigned to the calculated bands according to their energy and decay scheme. The very good agreement cannot be considered fortuitous. The original SM calculations using KB3 [2] differ from the present ones by at most hundred keV for any reported level and predict very similar em

moments within few percents. In the rest of the subsection we will refer principally to calculated level energies. The structure of the ^{48}Cr gs band was extensively discussed in the frame of SM [2]. As shown in Fig. 15 the gs band develops without band crossing up to the termination at 16^+ . This was also confirmed by CHFb calculations [2, 11]. In Fig. 16 the deformation parameter $\beta^*=0.31$ is assumed for the initial deformation, as previously made (Ref. [7]). The lowest 2-qp band is formed with $K^\pi=4^+$ by promoting one neutron or one proton from the $[321]3/2^-$ to the $[312]5/2^-$ orbital [8]. Its head is the yrare 4^+ which lies 2.3 MeV above the yrast 4^+ . It is rather unexpected that its Q_s value is less than half the rotor prediction (Fig. 16, lower panels), but anyhow the band develops rather regularly up to 8^+ . The predicted band shows SS and the $B(E2)$ to the fourth 4^+ level at 4975, built also mainly on a $1f_{7/2}^n$ configuration, is 163.0 efm^2 . These feature may indicate triaxiality which could explain the low Q_s value of the yrare 4^+ level. The yrare 2^+ level at 3624 keV has $Q_s=20.7 \text{ efm}^2$, consistent with a $K=2$ bandhead with a reduced deformation and it is connected with a $B(E2)$ rate of 104.0 efm^2 to the yrare 3^+ level at 5345 keV.

The antiparallel coupling gives rise to a 2-qp $K^\pi=1^+$ band. The lowest 1^+ level is predicted at 4844 keV. The corresponding experimental level is not known, but the prediction has to be considered reliable since in ^{50}Cr the yrast 1^+ is at 3629 keV, while theory gives the precise estimate of 3539 keV. A favoured connection of the yrast 1^+ level with the fourth 2^+ level at 4821 keV ($B(E2)=280.6 \text{ efm}^2$) is the only indication of an incipient $K^\pi=1^+$ band, which gets exhausted with the third 3^+ level at 5519 keV ($B(E2)=86.1 \text{ efm}^2$). All such calculated levels, without clear collective properties, are grouped on the rightmost side of Fig. 15.

As shown in the same figure, a 4-qp band with $K^\pi=8^+$ is predicted to start at an excitation energy of 7073 keV, about twice larger that for the $K^\pi=4^+$ band, being due to the simultaneous breaking of a proton and a neutron pair. Its Q_s value is 43.8 efm^2 , corresponding to $\beta^*=0.18$. The observed yrare 10^+ level decays mainly to the yrast 8^+ level with a 2644 keV transition and has a weak branch of 768 keV to the yrast 10^+ one [48]. This is expected by SM calculations for the member of the $K^\pi=8^+$ band. The yrare 12^+ is predicted to lie 2 MeV above the yrast one and to belong essentially to the $K^\pi=8^+$ band. At a similar excitation energy of the $K^\pi=8^+$ band also a 4-qp $K^\pi=2^+$ band may be expected of which however no evidence exists.

The γ -band is predicted to start at 3821 keV and to be well deformed (Fig. 16, lower panels). The peculiar nature of this band is revealed by its very fragmented wavefunction, where the $1f_{7/2}^n$ configuration contributes to less than 1% to the wavefunction of the lowest members, while in the gs band it has a 20% contribution and in the $K^\pi=4^+$ band a 37% one. Above 6^+ relevant mixing with the $K=4$ band occurs and also a large SS.

The Q_s values of the gs band approaching termination

are also very peculiar (Fig. 16, upper panels): they are consistent with an axially prolate description up to $I^\pi = 8^+$ but then suddenly become nearly zero at backbender level 12^+ and remain so for the levels 14^+ and 16^+ . If one repeats the calculations with the FPD6 interaction the behaviour is even more pronounced. CHFb [2, 11] and CNS [12] calculations estimate $\gamma \simeq -15^\circ$ at the backbending region. In Fig. 16 the CNS predictions are displayed for comparison. The axial description is good up to 6^+ , while the sudden decrease of Q_s above it requires some triaxiality with $\gamma \leq 0$. In fact, in the case of rotational collectivity Q_s is related to Q_o by eq. (1), which for $K=0$ becomes $Q_s = -Q_o I / (2I + 3)$ where:

$$Q_o = \frac{6}{\sqrt{5\pi}} Z e R_0^2 \beta \sin(30 + \gamma) \quad (7)$$

For negative values of γ Q_o decreases with respect to the axial symmetry, while an increase of $B(E2)$ values should occurs, according to eq. (2) and the relation:

$$Q_t = 2\sqrt{\frac{3}{5\pi}} Z e R_0^2 \beta \cos(30 + \gamma) \quad (8)$$

One should, however, comment that neither CNS [12] nor standard CHFb calculations [2] can reproduce well the backbending and the drastic reduction of Q_s at $I^\pi = 12^+$, which may suggest the bandcrossing with the 4-qp $K^\pi=2^+$ band, claimed in a PSM analysis [13]. However, the presence of that band, described in the PSM as little deformed, is excluded by SM and experimental data, as previously discussed. Since the yrare 12^+ level lies about 2 MeV higher than the yrast one, it has, on the contrary, to be concluded that what occurs is an intrinsic change of structure, not well described in a mean field approximation. In analogy to ^{49}Cr , the discontinuity at 12^+ can be interpreted as a sudden transition from collective to a nearly spherical shape, persisting at spins 14 and 16 and probably related with the $v=4$ termination at 12^+ , in absence of bandcrossing.

H. ^{52}Fe and ^{44}Ti

The experimental level scheme of ^{52}Fe is taken from NDS and from Ref. [39]. The fact that the terminating state 12^+ lies 424 keV below the 10^+ has a similar explanation as in ^{53}Fe . As shown in Fig. 17, the gs band in ^{52}Fe develops rather regularly up to spin 10^+ , with a smaller moment of inertia than ^{48}Cr . The calculated scheme was obtained with $s=3$. Clear correspondence is evident between experiment and theory, despite the somewhat worse agreement than for ^{48}Cr .

The presence of two close yrare levels 6^+ and 8^+ was already related to the 2-qp $K=6$ band, formed by the excitation of one neutron or one proton from the $[312]5/2^-$ to the $[303]7/2^-$ orbital [39]. The experimental yrare

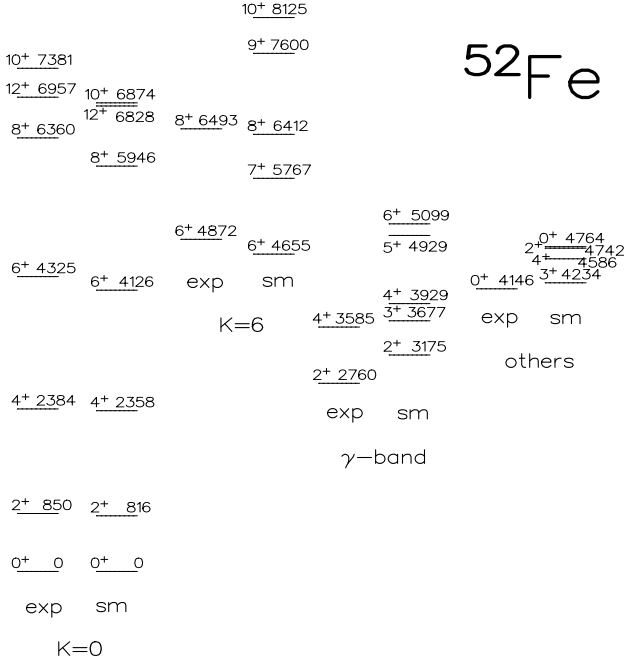


FIG. 17: Comparison of experimental positive parity levels in ^{52}Fe with SM predictions. ($s=3$)

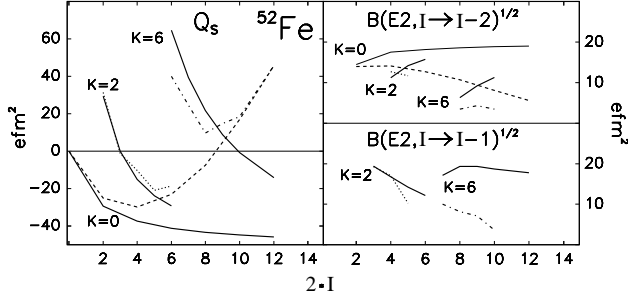


FIG. 18: Calculated em moments in ^{52}Fe . Rotor ($\beta^*=0.26$): solid lines, SM: dashed ($K=0$), dotted ($K=2$) and dot-dashed ($K=6$) lines. See text for details.

2^+ and 4^+ levels have, on the other hand, to be attributed to the $K^\pi=2^+$ γ -band, which lies about one MeV lower than in ^{48}Cr , in spite of the lower deformation. As in ^{48}Cr , the composition of γ -band is very fragmented, while in the $K^\pi=0^+$ and $K^\pi=6^+$ bands the $(f_{7/2})^{-4}$ configuration is dominant. The relevant offset for the γ -band with respect to calculations can, at least partially, be attributed to the space truncation. In fact it has been empirically observed that the excitation energies of the γ -band decrease remarkably with increasing s . The γ -band corresponds to a deformation $\beta^*=0.26$, as shown in Fig.18, and develops regularly up to $I=6$. There is, however, a mixing of about 15% with the gs band, as the yrare 4^+ level is predicted to be connected to the yrast 2^+ one by a $B(E2)$ rate of 40 efm^2 . For this reason one expects that the levels decays mainly to the yrast 2^+ level with a 2735 keV transition, while only

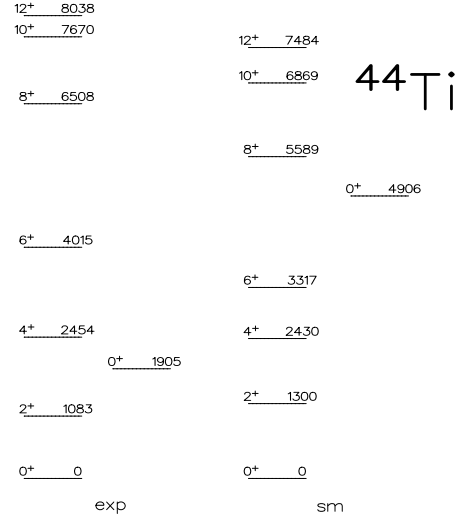


FIG. 19: Comparison of experimental gs band and yrare 0^+ levels in ^{44}Ti with SM predictions.

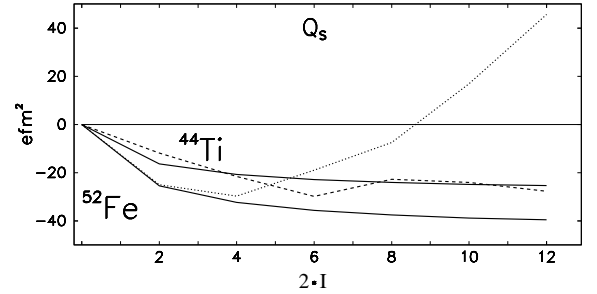


FIG. 20: Comparison between experimental and theoretical gs band Q_s values in ^{52}Fe ($\beta^*=0.23$) and ^{44}Ti ($\beta^*=0.21$).

by about one percent to the yrare 2^+ with a 825 keV transition.

Calculations predict the inversion between the yrast 12^+ and 10^+ levels, but their energy spacing is better reproduced by the FPD6 interaction, which, however, often predicts too large electric moments. Unfortunately $B(E2)$ values are not known with a sufficient precision in ^{52}Fe to discriminate between different effective interactions but it was shown in subsection A that the KB3G interaction gives a better agreement in the case of ^{54}Fe . It turns out that the KB3G interaction underestimate the relative binding energy of the terminating state in ^{52}Fe . The same occurs also for the $27/2^-$ terminating state in ^{51}Mn . It seems that the interaction KB3G needs an adjustment approaching the shell closure. The GXPF1 interaction gives similar results to the KB3G one.

The Q_s value of the 12^+ terminating state is calculated to be 47.1 efm^2 in agreement with the expected prolate non-collective shape associated to a 4-hole configuration and corresponding to a deformation $\beta^*=0.12$. Strong mixing of the gs band 6^+ and 8^+ levels with the corresponding members of the $K^\pi=6^+$ band is indicated by the experimental lifetimes and the connecting transitions [39]. Since large mixing makes the interpretation

difficult, the Q_s data of the $K=0$ and 6 bands represented in Fig. 18 were obtained in the $1f_{7/2}2p_{3/2}$ subspace ($s=0$), where the bands do not interfere much and the plots become similar to those in ^{51}Mn . The value of the terminating Q_s is slightly reduced to 46.8 efm^2 , while the β^* parameter decreases by about 8 % for the yrast 2^+ and 4^+ levels.

Using the Nilsson diagram for predicting a 4–qp band with the simultaneous excitation of both proton and neutron pairs, one gets $K = 12^+$, which is however the terminating state so that there is not a 4–qp band.

In Fig. 19 the experimental levels of the gs band of the cross–conjugate nucleus ^{44}Ti are compared with SM values. The agreement is poor. If one lifts up the SM spectrum by nearly one MeV in order to get the two 8^+ levels at the same height, the 0^+ , 2^+ and 4^+ levels appear to be more bounded than predicted by about one MeV. This is attributed to the strong influence of 2- and 4-hole configurations, as qualitatively discussed in Ref. [49], but quantitatively the question is still open. This interpretation is confirmed by the fact that the yrare 0^+ is predicted at 4906 keV, while it is observed at 1905 keV. The experimental one is clearly an intruder state which originates from 2- and 4-hole excitations. In this view, the levels 6^+ should be relative unaffected. Above $I=6$, which is the $v=2$ termination, the level spacing increases i.e. the opposite of a backbending seems to occur, which may be related with the onset of a change of regime. Looking back to ^{48}Cr one may wonder whether a small effect of the same type may explain the systematically lower level energies along the gs band at intermediate spins.

It is worthy to consider what would happen in absence of such intruder contributions. The Q_s behaviour of ^{52}Fe is compared with the one of the cross–conjugate nucleus ^{44}Ti in Fig. 20. The Q_s values do not mark the change of regime in ^{44}Ti , since they are anyhow negative as in ^{47}Ti . In this case the deformation parameter is reduced in ^{52}Fe in order to get a fit for the lower spins.

I. ^{50}Cr and ^{46}Ti

The $N=Z+2$ nucleus ^{50}Cr has been recently studied in detail [9]. The level scheme in Fig. 21 is essentially taken from that reference, even if some more calculated levels are now reported. The gs Q_s values are negative at low spin, being related to a collective prolate shape, while they become positive at the terminating level 14^+ (7.1 efm^2) as expected for an aligned–hole configuration. Bands with $K^\pi=4^+$ and $K^\pi=6^+$ were observed, which are expected by exciting one proton and one neutron from the $[321]3/2$ and $[312]5/2$ respectively. A $K=10$ band was also observed, which is obtained by breaking simultaneously both the neutron and the proton pairs. The em properties are displayed in Fig. 22. The smaller value Q_s value of the 6^+ level is presumably due to the mixing with the head of the $K=6$ band. This may ex-

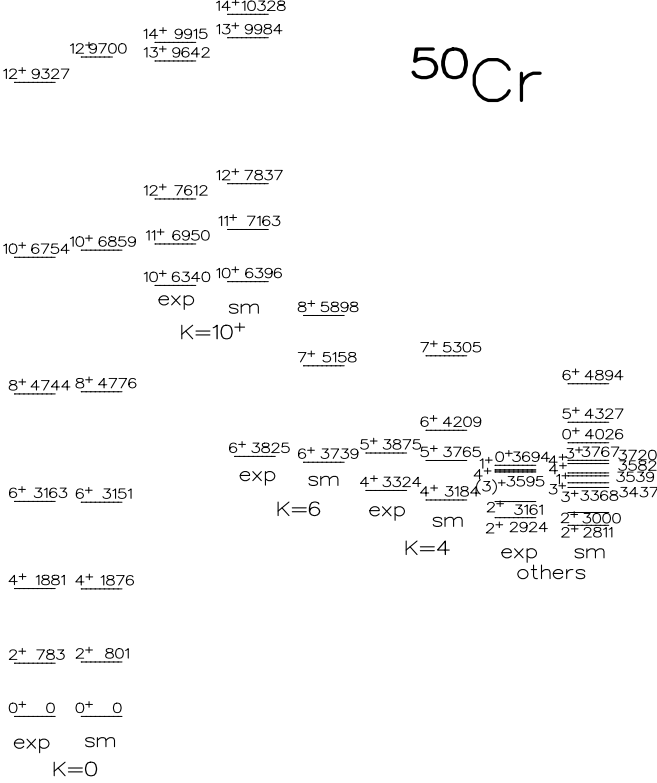


FIG. 21: Comparison of experimental positive parity and yrare 0^+ levels in ^{50}Cr with SM predictions.

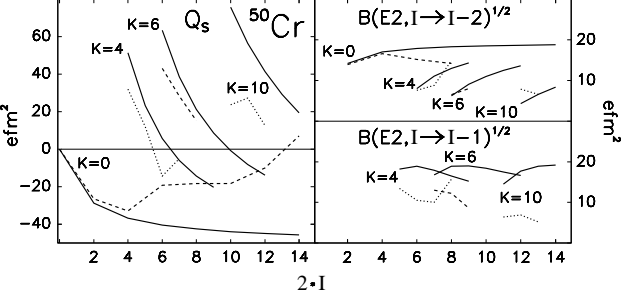


FIG. 22: Comparison between experimental and theoretical Q_s in ^{50}Cr . Rotor ($\beta^*=0.28$): solid lines, SM: dashed ($K=0$ and 6) and dotted ($K=4$ and 10) lines.

plain the large $B(M1)$ rate between the two levels [9]. The yrast 10^+ level is experimentally identified as the head of a $K=10$ band. SM calculations with the KB3G interaction predict a nearly 50 % mixing with the 10^+ level of the gs band, which has been commented to be an overestimate [9].

Levels not belonging to previous bands are reported on the rightmost side of Fig. 21. The level density is high both experimentally and theoretically, but the correspondence is good in particular for the two lower 2^+ levels.

In Ref. [9] the yrare 2^+ level observed at 2924 keV was

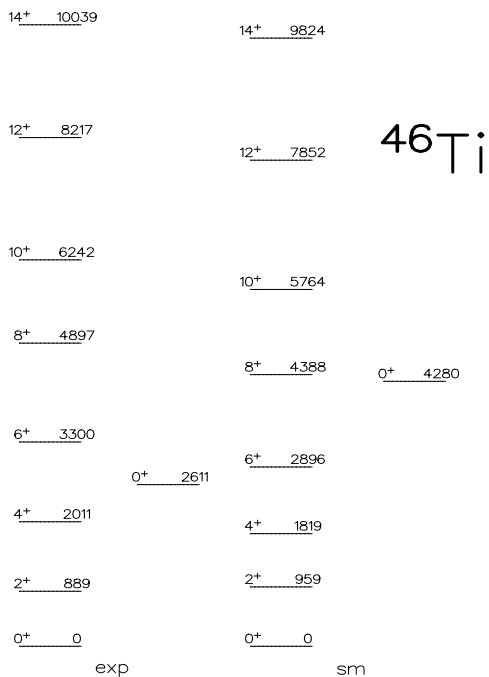


FIG. 23: Comparison of experimental gs band levels in ^{46}Ti with SM predictions.

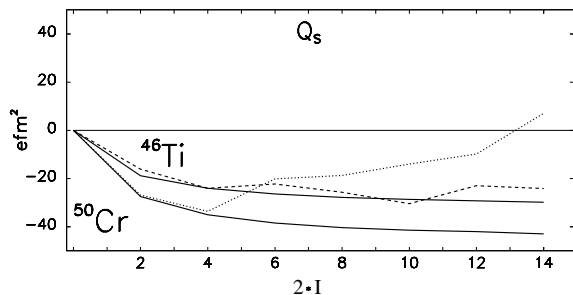


FIG. 24: Comparison between experimental and theoretical Q_s of ^{50}Cr ($\beta^*=0.28$) and ^{46}Ti ($\beta^*=0.23$).

suggested to be a member of $K=1$ band, following the antiparallel coupling of two unpaired nucleons. This is qualitatively confirmed by the present SM calculations since the level (calculated at 2811 KeV) has $Q_s=10.1 \text{ efm}^2$ and it is connected to the yrast 1^+ at 3629 keV (calculated at 3539 keV) and to the third 3^+ calculated at 3767 keV with $B(E2)$ rates of 241 and 157 efm^2 , respectively. The yrast 1^+ level is estimated to have a remarkable $B(M1)$ value of $0.35 \mu^2$ towards the gs so that it was observed in inelastic electron excitation (e, e') [50].

The positive Q_s of 29.5 efm^2 predicted for the third 2^+ level at 3161 keV (calculated at 3000 keV) makes it a candidate for the γ -bandhead. This is confirmed by the very fragmented wave function, but there should be, two 3^+ levels, at 3368 and 3437 keV, which strongly mix. It looks like as the $K=2^+$ mixes strongly with a $K=3^+$

band, having vibrational character too. This complex situation is not represented in Fig. 21 and it is not further discussed, owing to the lack of experimental information.

In Fig. 23 the experimental gs band of the cross-conjugate nucleus ^{46}Ti is compared with SM predictions. Similarly to ^{44}Ti , the low spin states of the gs band seem to mix with 2- and 4-hole core configurations, even if at a reduced scale. In fact, if we lift up the SM values by about 400 keV to get the 8^+ levels close, one deduces that the 0^+ , 2^+ and 4^+ levels are more bounded by about such value. Moreover the yrare 0^+ level is calculated at 4280 keV while it is observed at 2611 keV. The experimental $B(E2)$ values for the yrast 2^+ and 4^+ levels are larger than predicted [51], owing to the relevant contribution of the 2- and 4-hole configurations, while the 6^+ level is essentially unaffected as it results from the level scheme.

In Fig. 24 the Q_s values in ^{50}Cr are compared with the ones in its cross-conjugate nucleus ^{46}Ti . The comparison is made neglecting the core contribution in ^{44}Ti . The estimated deformation of ^{46}Ti is smaller ($\beta^* \simeq 0.23$) than in ^{50}Cr but still relevant at low spins. In ^{46}Ti the change from collective to non-collective regime seems to occur in conjunction with the backbending at $I^\pi = 10^+$, similarly to that at $I^\pi = 12^+$ in ^{48}Cr . A major difference is that there is not a simple relation with a termination in a seniority subspace. It seems that the change of regime does not necessarily start at a seniority subspace termination, as previously observed for ^{47}Ti .

IV. UNNATURAL PARITY BANDS

The shell model description of unnatural parity bands requires to consider simultaneously two major shells and, implicitly, severe space truncations. Moreover, it is difficult to select a good effective interaction. In spite of these severe requirements, reasonable and even satisfactory agreement was achieved in several cases. It is too early for a detailed discussion so that only a brief summary will be presented, limited to odd- A nuclei.

Low-lying $I^\pi = 3/2^+$ and $1/2^+$ levels, interpreted as heads of the bands having $[202]3/2^+$ and $[200]1/2^+$ Nilsson configurations, were observed in $N = Z+1$ nuclei ^{45}Ti , ^{47}V , ^{49}Cr and ^{51}Mn . Such 1-hole configurations are selectively populated in pickup reactions: the heads of the $K^\pi=3/2^+$ band were identified at 293, 260, 1982 and 1817 keV, respectively, while the heads of the $K^\pi=1/2^+$ band at 1565, 1660, 2578 and 2276 keV, respectively. The assignments in ^{51}Mn are based on the decay scheme and systematics.

SM calculations were performed mostly for the $K^\pi=3/2^+$ band and in this case the pf configuration space was enlarged to include a hole in the $1d_{3/2}$ orbital. These bands have generally a deformation different from that of the gs one. Recently, also the $K^\pi=1/2^+$ band in ^{49}Cr was described, but for this, the extension to the $2s_{1/2}$ orbital was necessary [17]. In fact, the $[200]1/2^+$ Nilsson orbital contains a large contribution from the

spherical $2s_{1/2}$ orbital. Several effective interactions have been used, some of them being derived from that used in Ref. [52] by adjustment of monopole terms.

The high- K bands predicted by SM at the lowest energy in such configuration space have $K^\pi=9/2^+$, $11/2^+$, $13/2^+$ and $15/2^+$ in ^{45}Ti , ^{47}V , ^{49}Cr and ^{51}Mn , respectively. They are produced by promoting a $[202]3/2^+$ nucleon to the first empty orbital and the recoupling of the three unpaired nucleons to the maximum K value, obviously, with the necessary mixing of proton and neutron holes in order to keep isospin conservation. They can be also represented as the configurations $\pi d_{3/2}^{-1} \otimes ^{46}\text{V}(K=3, T=0)$, $\nu d_{3/2}^{-1} \otimes ^{48}\text{V}(K=4, T=1)$, $\pi d_{3/2}^{-1} \otimes ^{50}\text{Mn}(K=5, T=0)$ and $\nu d_{3/2}^{-1} \otimes ^{52}\text{Mn}(K=6, T=1)$, respectively.

The dipole band $K^\pi=13/2^+$ in ^{49}Cr is yrast and the observed first five members are well reproduced by SM calculation [15]. Its band termination is predicted by SM at $33/2^+$. Evidence was also found of the $K^\pi=7/2^+$ partner band, obtained from an antiparallel coupling in the $\nu d_{3/2}^{-1} \otimes ^{50}\text{Mn}(I=5, T=0)$ configuration [17].

Members of the dipole band $K^\pi=9/2^+$ in ^{45}Ti have been also recently observed from $I^\pi = 17/2^+$ up to the termination at $I^\pi = 33/2^+$ [53]. The reason why members with spin value lower than $17/2^+$ are not observed may be that the 3^+ and 5^+ terms are rather close to the 7^+ level in ^{46}V , so that the decay-out is favoured by the transition energy. The SS reflects that of the $K^\pi=3^+$ band in ^{46}V [20], where it becomes larger approaching the band termination. For this reason dipole transitions and the unfavoured signature members were not observed both in the $K=3$ band in ^{46}V and in the $K^\pi=9/2^+$ band in ^{45}Ti .

Unfortunately, non yrast structures are not known in ^{47}V , so that also the $K^\pi=11/2^+$ band was not observed.

In ^{51}Mn the $K^\pi=15/2^+$ band was also not observed but the experimental situation is intriguing. Recently, a positive parity band was observed up to $39/2^+$ [43] and attributed to the $\nu g_{9/2} \otimes ^{50}\text{Mn}(K=5, T=0)$ configuration, which is intruder with respect to the so far considered configuration space. The termination in the configuration space is $39/2^+$, in agreement with observation. Since ^{50}Mn is prolate, the decoupled $[440]1/2^+$ intruder orbital should be considered. Assuming the coupling of the band $^{50}\text{Mn}(K=5, T=0)$ with the $9/2^+$ state of the decoupled $1g_{9/2}$ band, one would expect a $19/2^+$ bandhead. Dipole transitions connecting the unfavoured signature levels were not observed above $27/2^+$. This seems to reflect the fact that unfavoured signature members were not observed in ^{50}Mn above $I=9$, because of the large SS [54]. The situation is similar to that discussed for the $K=9/2$ band in ^{45}Ti .

The reason why the predicted partner quadrupole band $\pi g_{9/2}^{-1} \otimes ^{50}\text{Cr}(K=0, T=1)$, terminating at $I^\pi = 37/2^+$, is not observed, may be that its bandhead $9/2^+$ is expected at similar energies as the $19/2^+$ one and it is thus largely non yrast. There is also an explanation

of the reason why the predicted “extruder” $K^\pi=15/2^+$ $\nu d_{3/2}^{-1} \otimes ^{52}\text{Mn}(K=6, T=1)$ band is not observed. An estimate of its excitation energy is made considering that the IAS level of the 6^+ gs level of ^{52}Mn in ^{52}Fe is at 5655 KeV. Adding this value to the excitation energy of the yrast $3/2^+$ in ^{51}Mn of 1817 keV one gets 7472 keV, which is similar to the excitation energy of the lowest terms of the observed band. Its termination is $25/2^+$, well below $39/2^+$, so that the flux generated at high spin is efficiently captured by the “intruder” band, while little goes into the “extruder” one.

Large (τ, α) spectroscopic factor with $\ell_n=0$ and $\ell_n=2$ were observed in ^{53}Fe for the levels at 3400 and 2967 keV, respectively, so that they are identified as the $3/2^+$ and $1/2^+$ states dominated by the $1d_{3/2}$ and $2s_{1/2}$ orbitals, respectively, which appear to be inverted.

As mentioned, unnatural parity bands were observed also in several even-even and odd-odd nuclei and were described by lifting a $[202]3/2^+$ nucleon to the pf space [52]. Satisfactory agreement was achieved in even-even ^{48}Cr , ^{50}Cr and ^{46}Ti [7, 17, 46], as well as in odd-odd nuclei ^{46}V , ^{48}V [20, 21].

V. CONCLUSIONS

A critical review is presented of the collective phenomena predicted by SM in several odd- A and even-even nuclei of the $1f_{7/2}$ shell, for natural parity levels up to the band termination in a $f_{7/2}^n$ space. Deformation alignment (strong coupling) occurs at low excitation energy in odd- A nuclei in the second half of the shell, while evidence of rotational alignment is limited to nuclei in the first half of the shell.

Evidence of vibrational γ -bands is found in both ^{48}Cr and ^{52}Fe . The mixing of the gs band of ^{52}Fe with sidebands is better outlined.

The Nilsson diagram predicts correctly the lowest sidebands in odd- A nuclei. The lowest 3-qp sidebands in ^{49}Cr and ^{51}Mn have $K^\pi=13/2^-$ and $17/2^-$ respectively, as they are described by the excitation of one nucleon from the $[321]3/2^-$ to $[312]5/2^-$ orbital or from the $[312]5/2^-$ to the $[303]7/2^-$ orbital, respectively. Only in the second case a clear crossing with the gs band occurs, while the backbending of ^{49}Cr gs band at $19/2^-$ stems probably from a smooth band termination in the $v=3$ subspace. This conclusion shows that in general a backbending is not necessarily caused by bandcrossing and that the statement based on PSM calculations that backbendings in ^{49}Cr and ^{51}Mn are both caused by the crossing with a 3-qp $K^\pi=7/2^-$ band [55] is untenable.

The collective rotation is damaged in $N=Z+1$ nuclei ^{47}V , ^{49}Cr and ^{51}Mn above $I=13/2$, indicating a change of regime.

Similarly to ^{49}Cr , the understanding of the backbending at $I=12$ in ^{48}Cr , cannot be achieved in the frame of the standard mean field approximation. In CHFb, only a treatment sensible to details of the effective two

body interaction, can predict a backbending at $I^\pi = 12^+$ [11]. The evolution of Q_s points to a sudden change of regime from collective to nearly spherical, in absence of any bandcrossing. Experimental data and SM calculations exclude, in fact, a crossing of the ^{48}Cr gs band with a 4-qp $K=2$ band, which served in the PSM to explain the experimental backbending [13].

What seems principally to occur is the competition between the pairing and the quadrupole terms of the nucleon–nucleon interaction. With increasing spin, the number of interacting particles in the $2p_{3/2}$ orbital decreases. Consequently the rotational collectivity induced by the quadrupole term also decreases. The pairing interaction becomes, therefore, relatively more important, leading in several cases to a rapid change from collective to non–collective regime. This change, often correlated with a termination in a seniority subspace, occurs in different manners, not yet understood.

The gs bands in nuclei lying in the second half of the $1f_{7/2}$ shell, as ^{51}Mn , ^{51}Cr , ^{52}Fe and ^{53}Fe , become prolate non–collective approaching the termination, but the states are not pure $1f_{7/2}^n$, as commonly believed, as the other orbitals of the pf configuration space contribute to a large extent, increasing the state deformation.

A review of non natural parity structures is also presented.

The $1f_{7/2}$ region is a unique testing bench for the study of the origin of nuclear quadrupole deformation. There are more mechanisms of generating deformation but what

occurs in the $1f_{7/2}$ shell is a well understood case, where most of the game is played by the orbitals $1f_{7/2}$ and $2p_{3/2}$. SM is a precise microscopic probe of any particle–alignment mechanisms. It predicts accurate observables, which react to most structural effects, where other models may fail. Since SM provides very reliable values for the observables in the $1f_{7/2}$ shell, nuclear models based on the deformed meanfield approximation should calibrate their predictions on the SM ones. In particular, those models which assume a fixed deformation cannot be considered reliable in this region. While the $1f_{7/2}$ region may appear as a garden for SM calculations, it is rather a mined field for meanfield models.

The general picture presented appears to be well grounded, but new experimental data are required to confirm the coexistence of rotational and vibrational degrees of freedom predicted by SM. For this purpose full spectroscopy using light–projectiles induced reactions appears to be the best chance in order to measure accurately the properties of some non-yrast levels of rather low spin.

Acknowledgments

This theoretical survey follows a long experimental work performed at LNL. Several discussions with coworkers are acknowledged.

-
- [1] E. Caurier, A.P. Zuker, A. Poves and G. Martinez–Pinedo, *Phys. Rev. C* **50**, 225 (1994);
 - [2] E. Caurier *et al.*, *Phys. Rev. Lett.* **75**, 2466 (1995);
 - [3] G. Martinez–Pinedo, A. Poves, L.M. Robledo, E. Caurier, F. Novacki and A.P. Zuker, *Phys. Rev. C* **54**, R2150 (1996);
 - [4] G. Martinez–Pinedo, A.P. Zuker, A. Poves and E. Caurier, *Phys. Rev. C* **55**, 187 (1997);
 - [5] S.M. Lenzi *et al.*, *Z. Phys.* **A354**, 117 (1996);
 - [6] S.M. Lenzi *et al.*, *Phys. Rev. C* **56**, 1313 (1997);
 - [7] F. Brandolini *et al.*, *Nucl. Phys.* **A642**, 387 (1998);
 - [8] F. Brandolini *et al.*, *Experimental Nuclear Physics in Europe*, Seville, Spain, 1999. Editors B. Rubio, M. Lozano and W. Gelletly, AIP Conf. Proceedings 495, 1999, pag. 189;
 - [9] F. Brandolini *et al.*, *Phys. Rev. C* **66**, 021302 (2002);
 - [10] S.M. Lenzi *et al.*, *Phys. Rev. Lett.* **87**, 122501 (2001)
 - [11] T. Tanaka, K. Iwasawa and F. Sakata, *Phys. Rev. C* **58**, 2765 (1998);
 - [12] A. Juodagalvis, I. Ragnarsson and S. Aberg, *Phys. Lett.* **B477**, 66 (2000);
 - [13] K. Hara, Y. Sun and T. Mizusaki, *Phys. Rev. Lett.* **83**, 1922 (1999);
 - [14] A. Juodagalvis and S. Aberg, *Phys. Lett.* **B428**, 227 (1998);
 - [15] F. Brandolini *et al.*, *Phys. Rev. C* **60**, R041305 (1999);
 - [16] F. Brandolini *et al.*, *Nucl. Phys.* **A693**, 571 (2001);
 - [17] F. Brandolini *et al.*, to be published;
 - [18] E. Caurier, G. Martinez–Pinedo, F. Novacki, A. Poves and A.P. Zuker, arXiv:nucl-th/0402046 (2004);
 - [19] A. Poves, J. Sanchez–Solano, E. Caurier and F. Novacki, *Nucl. Phys.* **A694**, 157 (2001);
 - [20] F. Brandolini *et al.*, *Phys. Rev. C* **64**, 044307 (2001);
 - [21] F. Brandolini *et al.*, *Phys. Rev. C* **66**, 024304 (2002);
 - [22] W.A. Richter, M.G. van der Merwe, R.E. Julies and B.A. Brown, *Nucl. Phys.* **A523**, 325 (1991);
 - [23] T. Otsuka, M. Honma and T. Mitsuzaki, *Phys. Rev. Lett.* **81**, 1588 (1998);
 - [24] M. Honma, T. Otsuka, B.A. Brown and T. Mizusaki, *Phys. Rev. C* **69**, 034335 (2004);
 - [25] M. Hasegawa and K. Kaneko, *Phys. Rev. C* **59**, 1449 (1999);
 - [26] E. Caurier, Shell Model code ANTOINE, IRES, Strasbourg 1989–2002;
 - [27] E. Caurier and F. Novacki, *Acta Physica Polonica* **30**, 705 (1999);
 - [28] A. Zuker, J. Retamosa, A. Poves and E. Caurier, *Phys. Rev. C* **52** R1742 (1995);
 - [29] A. Bohr and B.R. Mottelson, *Nuclear Structure* (Benjamin, New York, 1975) Vol. 2, pag. 45.
 - [30] K.E.G. Löbner, M. Vetter and V. Hönl, *Nuclear Data Tables* **7**, 495 (1970);
 - [31] S.E. Larson, G. Leander and I. Ragnarsson, *Nucl. Phys.* **A307**, 189 (1978);
 - [32] S.J. Williams *et al.*, *Phys. Rev. C* **68**, 011301 (2003);
 - [33] W.J. Gerace and A.M. Green, *Nucl. Phys.* **113**, 641

- (1968);
- [34] J.M. Espino *et al.*, LNL Annual Report 2001, pag 10;
 - [35] I. Ragnarsson, V.P. Jansen, D.B. Fossan, N.C. Schmeing and R. Wadsworth, Phys. Rev. Lett. **74**, 3935 (1995);
 - [36] B.G. Dong and H.C. Guo, Eur. Phys. J. **A17**, 25 (2003).
 - [37] S. Aberg, Nucl. Phys. **A306**, 89 (1978);
 - [38] J.A. Sheik, D.D. Warner and P. van Isacker, Phys. Lett. **B443**, 1 (1998);
 - [39] C.A. Ur *et al.*, Phys. Rev. C **58**, 3163 (1998);
 - [40] B. Bengtsson and S. Frauendorf, Nucl. Phys. **327**, 139 (1979);
 - [41] C. Rusu *et al.*, Phys. Rev. C **69**, 024307 (2004);
 - [42] J.A. Cameron *et al.*, Pys.Rev. C **58**, 808 (1998);
 - [43] J. Ekman *et al.*, Phys. Rev. C **70**, 014306 (2004);
 - [44] J. Ekman *et al.*, Eur. Phys. J. **A9**, 13 (2000);
 - [45] M.A. Bentley *et al.*, Pys.Rev.C **62**, 051303R (2000);
 - [46] F. Brandolini, Eur. Phys. J. **A20**, 139 (2004);
 - [47] K. Jessen *et al.*, Phys. Rev. C **68**, 047302 (2003);
 - [48] C.A. Ur, Eur. Phys. J. **A20**, 113 (2004);
 - [49] C.D. O'Leary *et al.*, Phys. Rev. C **61**, 064314 (2000);
 - [50] A. Willis *et al.*, Nucl. Phys. **A499**, 367 (1989).
 - [51] F. Brandolini *et al.*, submitted to Phys. Rev. C;
 - [52] A. Poves and J. Sanchez-Solano, Phys. Rev. C **58**, 179 (1998);
 - [53] P. Bednarczyk *et al.*, Eur. Phys. J. **A20**,45 (2004);
 - [54] C.E. Svenson *et al.*, Phys. Rev C **58** R2621 (1998):
 - [55] V. Velasquez, J.G. Hirsch, Y. Sun, Nucl. Phys. **A686**, 129 (2001);